Calibration of a Magnet used for Hall Probe Calibration in Mu2e Experiment

Summer Internship 2016

Daniele Marchetti

Supervisor: Thomas Strauss

Co-Supervisor: Luciano Elementi

Co-worker: Francesco Restuccia

Fermilab Technical Division – U.S. Department of Energy

Contents

1 Introduction

Mu2e is an experiment with the goal of measuring the ratio of the rate of the neutrino-less, coherent conversion of muons into electrons in the field of a nucleus, relative to the rate of ordinary muon capture on the nucleus, with a single event sensibility of 2.87×10^{-17}. The experiment consists of a superconducting solenoid system (Figure 1): a Production Solenoid, an S-shaped Transport Solenoid and a Detector Solenoid [1]. The magnetic field of the Detector Solenoid must be mapped with a precision of better than 10^{-4} T, in order to perform the precision momentum analysis of particles that traverse the tracker and calorimeter of the Detector. Hall Probes will be used to get a 3D map of the field and Nuclear Magnetic Resonance (NMR) Probes will be used to measure the absolute field value [2]. To perform the field mapping, Hall Probes need to be calibrated in the intended measurement range at a known homogeneous magnetic field much better than 10^{-4} T [3].

The GMW 3474-140/280 250 mm Electromagnet (Figure 2) would be used to calibrate the Hall Probes. Our task is study and test the magnet to meet the magnetic field requirements needed for the Hall Probe calibration: a field homogeneity much better than 10^{-4} T in a region of 2 cm $\times$ 2 cm, large enough to hold the Hall Probe and to allow the movement of it during the calibration; a field stability over time to ensure the measurement repeatability [4]. These are hard constraints because a lot of factors, such as pole skewness, magnetic hysteresis and iron saturation, can decrease the field homogeneity and stability, compared to the ideal case.

At first we studied the magnet design using the manual, to understand the magnet operation. Then we created a model of the magnet and we simulated the magnetic field to see at prior if the magnet can meet the requirements in the ideal case; we simulated also the field distortion due to a non ideality in the model, in particular the pole skewness, and we showed that a particular procedure, called shimming, can compensate the field distortion and increase the field homogeneity. Subsequently we mapped the magnetic field using an NMR Probe mounted on a 2-axis motion robot using LabVIEW interface. We analyzed data of several mapping, understanding the behavior of the magnet: the pole skewness, the hysteresis phenomena, the correlation between the field and supply current, the iron saturation and the field stability over time. Finally we applied solutions to decrease the effect of such non idealities and we concluded that one can achieve the requirements for the Hall Probe calibration stabilizing the power supply and then performing the shimming procedure.

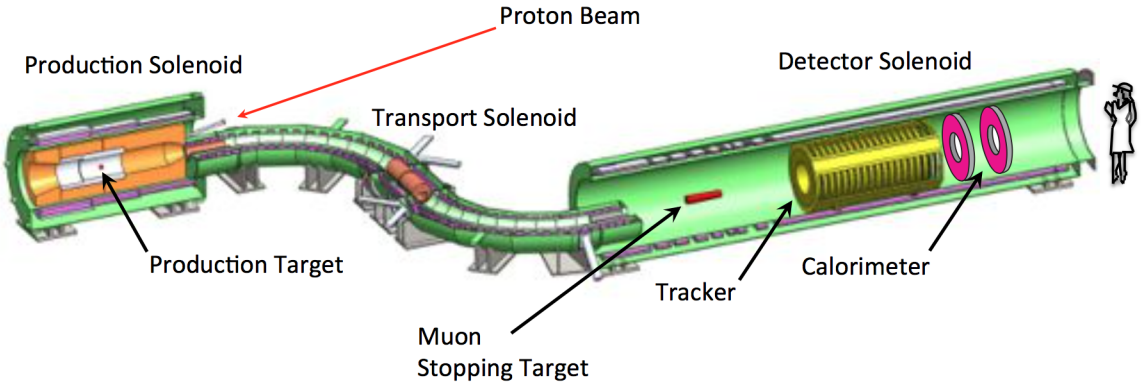

Figure 1: Solenoid system in Mu2e experiment.

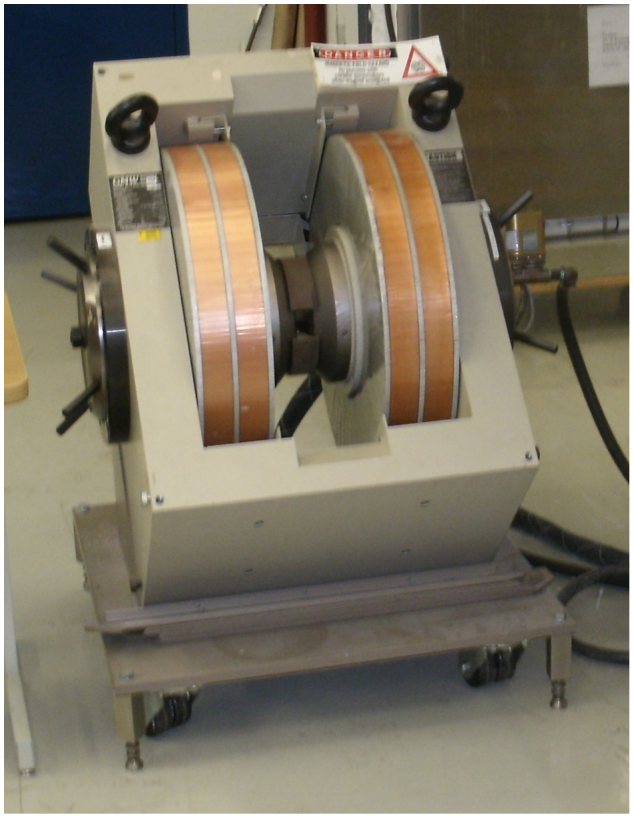

Figure 2: GMW 3474-140/280 250 mm Electromagnet.

2 Magnet Design

[5] GMW 3474 is a dipole electromagnet typically used when high field and high uniformity are needed. The magnet main components are a couple of coils, poles, pole caps and an iron yoke (Figure 3). The current flows into the coils and generates a magnetic field that magnetize poles and yoke, resulting in a high magnetic field in the magnet center between the two poles. Poles are cylindrical and have a diameter of 250 mm but on the pole surface can be mounted pole caps with different geometry and face diameter. Pole cap geometry is a decisive factor in determining the field. In fact, we used pole caps with two tapered edges (45° and 30°) and face diameter of 150 mm (Figure 4) in order to increase the field magnitude and homogeneity in the magnet center (Figure 5). The pole gap can be manually adjusted from 0 to 160 mm; Figure 6 shows the field Vs current plot for different values of pole gap and it is clear that decreasing the pole gap, the magnetic field at a given supply current value is higher. Therefore, we used a pole gap of 50 mm, a good trade off between available space in the center and field magnitude. Figure 6 shows also that field and supply current have a linear relationship, but a field saturation occurs increasing the current over a certain value, that depends on the pole gap.
It is important to note that in the magnet used in this project coils are connected in parallel; instead, the characteristic curves taken from the manual are referred to a magnet with coils connected in series: this is the reason of the difference between plot values shown by the manual and our measured values.
A water cooling system is used to cool the coils. The first coil in which the water flows may be hotter than the second one. Since coil resistance depends on temperature, the current flowing in each coil may be different. This asymmetry can affect the magnetic field.

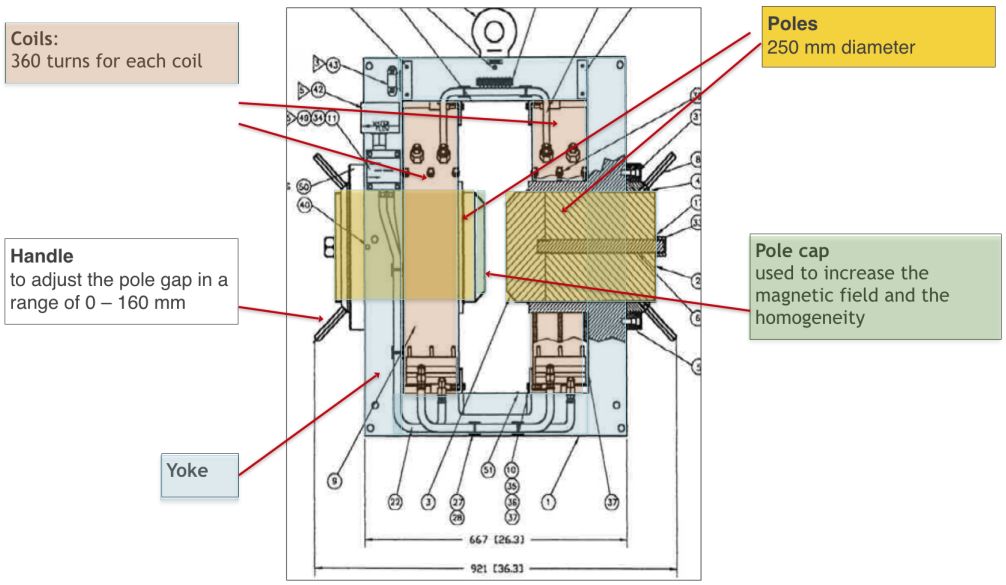

Figure 3: Rear view of the magnet, taken from the manual.

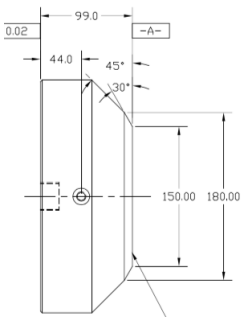

Figure 4: Pole cap.

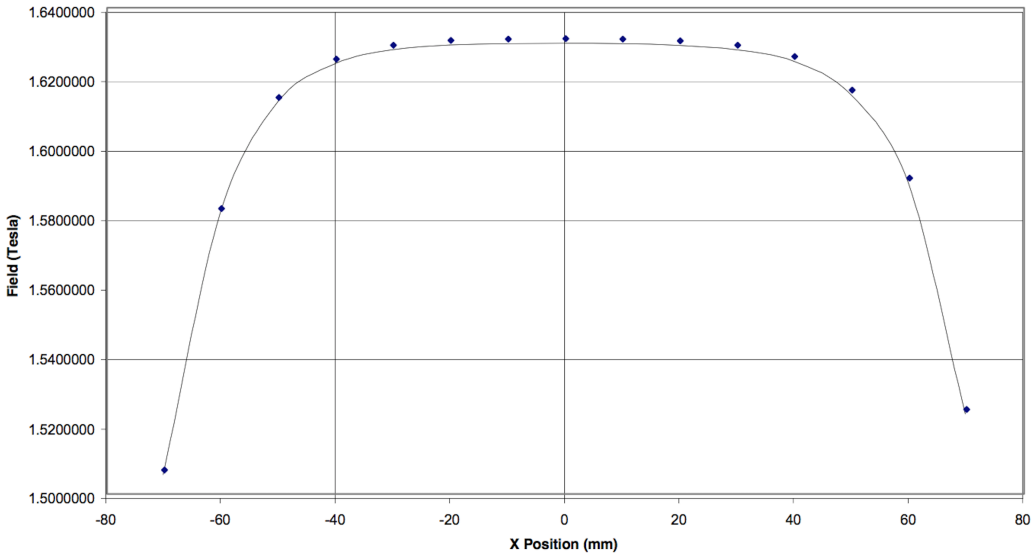

Figure 5: Magnetic field along an X direction line in the magnet center, with 100 A coil current and 50 mm pole gap.

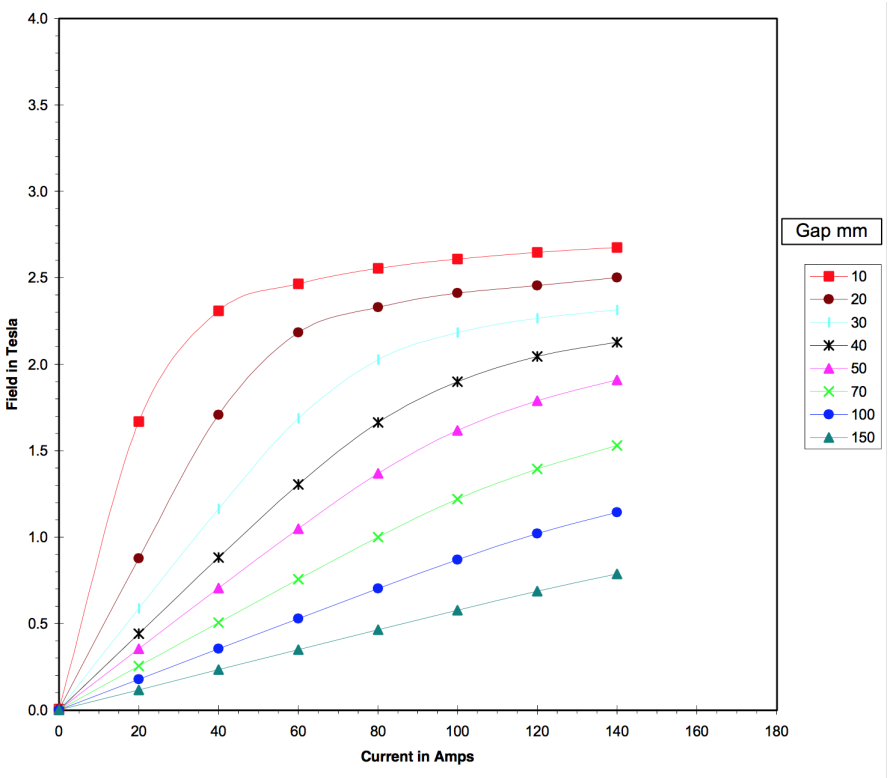

Figure 6: Magnetic field Vs supply current for different values of pole gap.

3 COMSOL Simulations

COMSOL is a software that uses the Finite Element Method to solve and simulate physics and engineering problems, as the mechanic deformation of a stressed structure or the fluid flow inside a tube. It allows also to include different physics in one model [14]. In our case we used the electrical AC/DC module to simulate the magnetic field generated by the electromagnet. We started with simple 2D and 2D axisymmetric model and finally we implemented a more realistic 3D model, of which we show the simulation results. At first the magnetic field was simulated in the ideal case, that is without taking into account hysteresis and saturation effects, and considering perfectly aligned poles. Then a pole skewness was included in the model to simulate the field distortion. Finally it was simulated the effect of shimming, a procedure commonly used to compensate the field distortion and to increase the homogeneity. Particular attention was paid in showing the simulation results over the 2 cm $\times$ 2 cm region in the magnet center, needed for the Hall Probe calibration.

3.1 2D Model

2D Model has this name because the object can be modeled representing only a section of it (Figure 7). It does not mean that the model is planar; rather the section is extended by the simulator in the third dimension orthogonal to the plane of a quantity that can be set. It is not so realistic because not all regions of the magnet section have actually the same depth. Coils are not included, it was modeled only a permanent magnetization of poles.

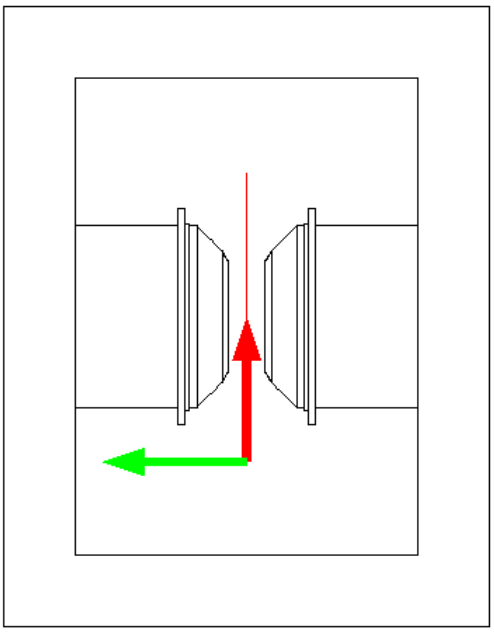

Figure 7: 2D Model with a red cut line in the magnet center.

3.2 2D Axisymmetric Model

Coils, poles and pole caps of the actual magnet have a cylindrical symmetry, so this explains the use of a 2D axisymmetric model. The object can be modeled representing a section that is virtually rotated along the symmetry axis (Figure 8). The only thing that jeopardizes the model is that the yoke has not really a cylindrical symmetry.

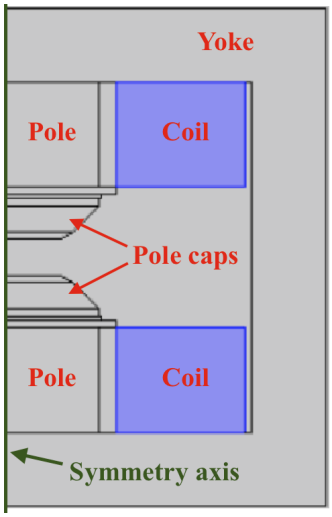

Figure 8: 2D axisymmetric model.

3.3 3D Model

3D Model is more realistic than the previous two because it takes into account the geometry of all magnet components (Figure 9), the current generated by coils and iron magnetization. We simulated the magnetic field using a finer mesh in the magnet center and courser mesh outside, in order to increase the simulation precision in the region of interest but at the same time to restrain the simulation time.

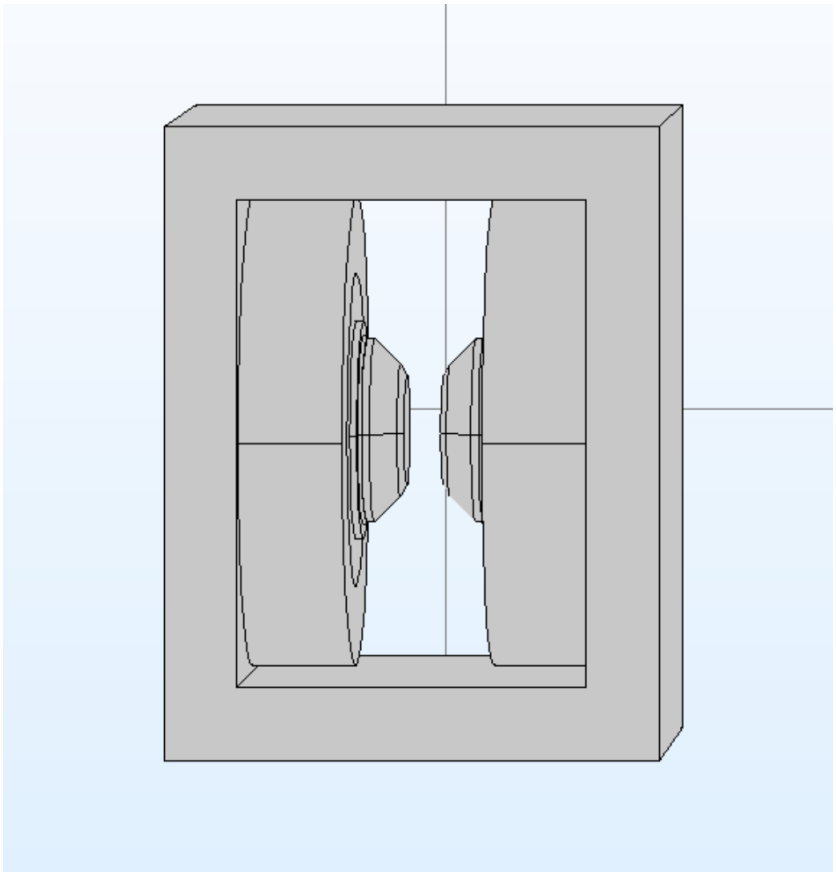

Figure 9: 3D Model.

Ideal case

Figure 10 compares the magnetic field simulated in the ideal case along a Z direction line in the magnet center (Figure 11) with that shown by the manual with 100 A supply current, 50 mm pole gap and coil connected in series. The simulation reproduces well the behavior of the magnet.

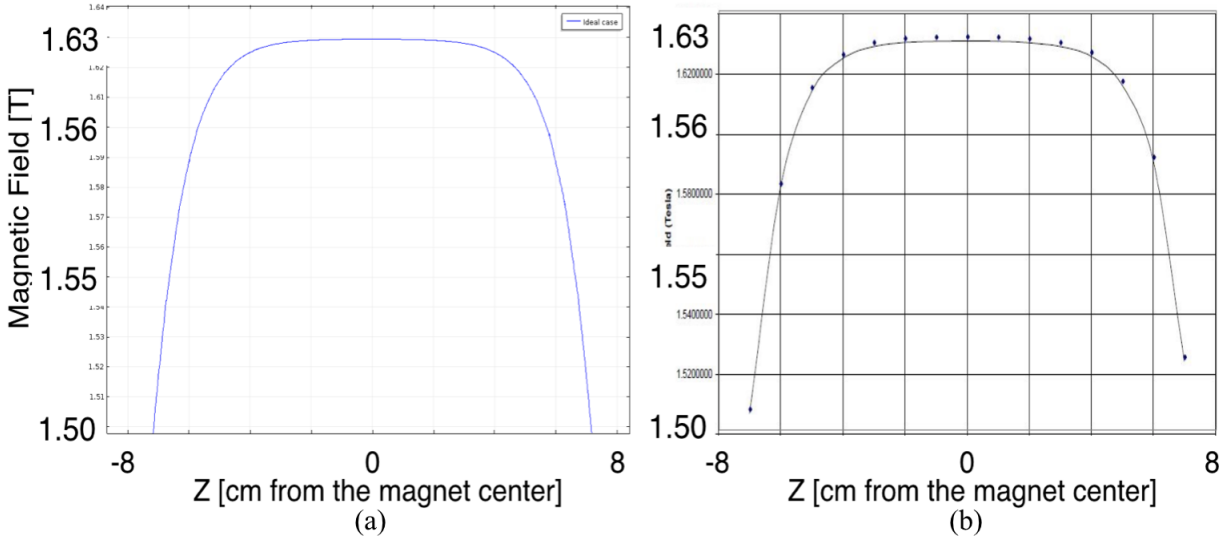

Figure 10: Magnetic field along a Z direction line in the magnet center: (a) by the simulation, (b) by the manual. 100 A Supply current, 50 mm pole gap, coil connected in series.

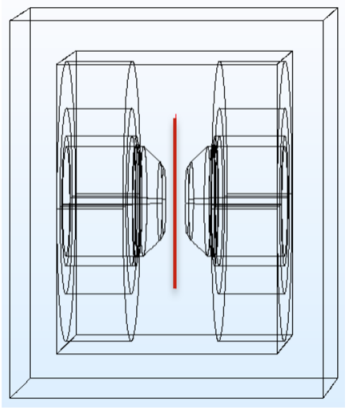

Figure 11: Z direction line in the magnet center, red colored, along which the magnetic field is shown.

Pole skewness

A pole skewness of 0.5° was included in the model; the field was compared with the ideal case (Figure 12). Figure 13 shows the pole skewness, higher than implemented, in order to see the direction of the skewness. In the ideal case the field homogeneity is minor than 10^{-4} T over 2 cm. The pole skewness decreases the homogeneity to 6×10^{-3} T over the same region. The field is higher where poles are closer and smaller where poles are less closer because of skewness.

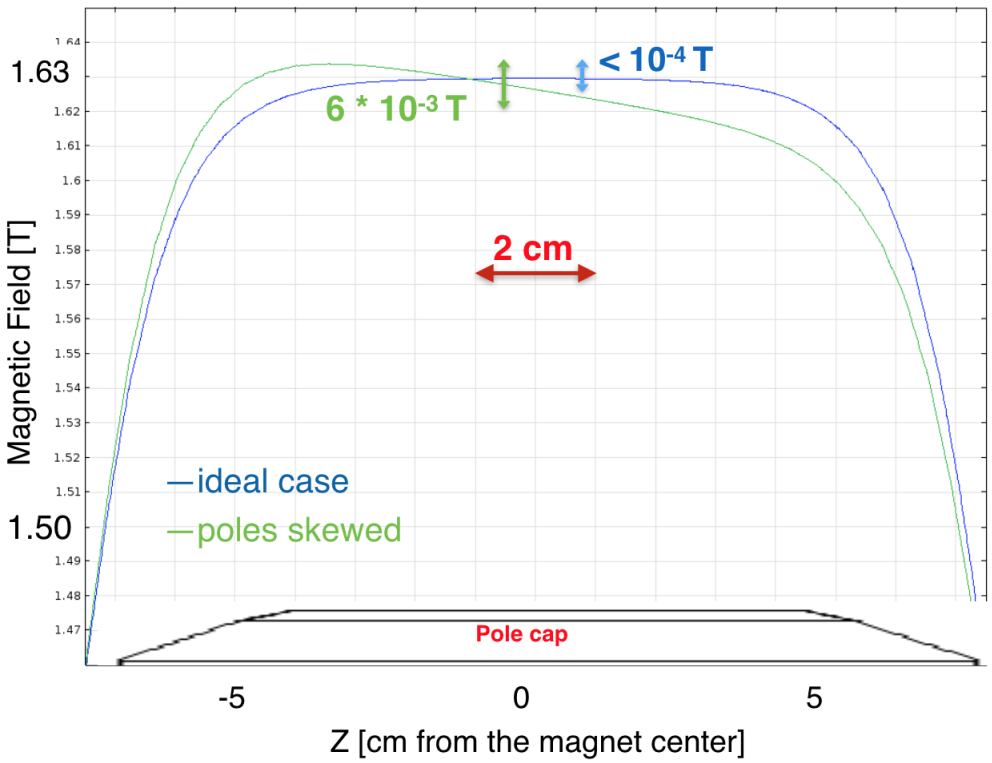

Figure 12: Magnetic field along a Z direction line in the magnet center, in the ideal case and with 0.5° pole skewness. Both cases were simulated using 100 A supply current, 50 mm pole gap and coil connected in series. The pole cap is not in scale.

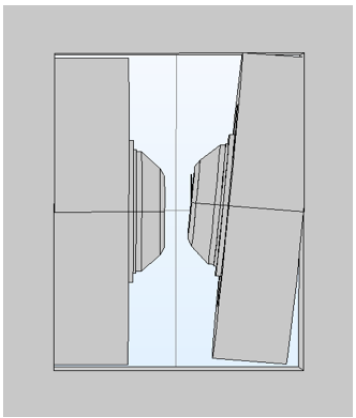

Figure 13: Pole skewness, higher than implemented.

Shimming

Shimming is a trial and error procedure commonly used to increase the magnetic field homogeneity. Shims are thin metal strips that added on the magnet surface, change the geometry and compensate the field. It is a trial and error procedure because it consists in mapping the field, putting the shims, mapping the field again and repeating these steps until the required homogeneity is achieved. Shims were modeled as thin iron strips of 430 μm × 3 cm × 1 cm, added on the pole surface on the side where poles are less closer, in order to compensate the field. After several simulations we found a shim configuration (Figure 14) that increases the field homogeneity from 6×10^{-3} T to a value $< 10^{-3}$ T over 2 cm, as shown in Figure 15.

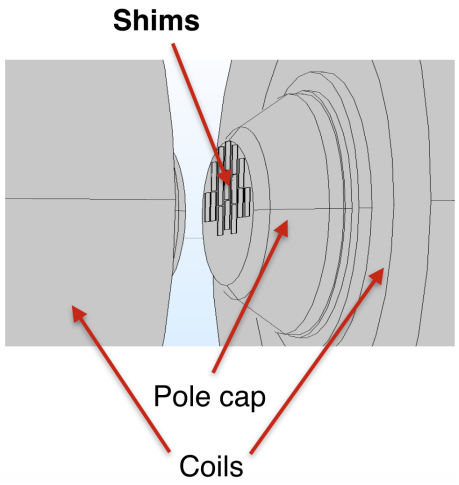

Figure 14: Shims positioning on the pole surface.

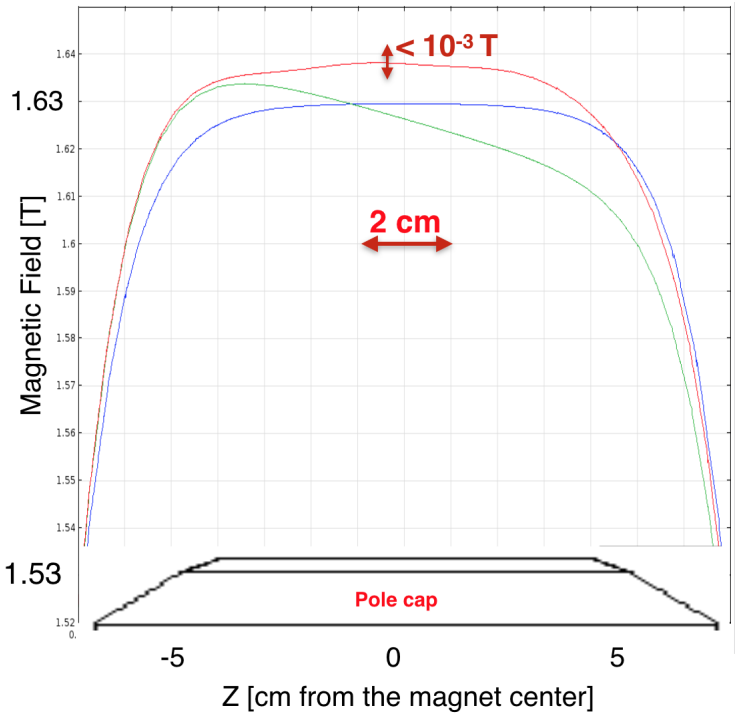

Figure 15: Magnetic field along the Z direction line in the magnet center in three different cases: ideal, with 0.5° pole skewness and with shimming procedure. All cases were simulated using 100 A supply current, 50 mm pole gap and coil connected in series. The pole cap is not in scale.

3D Simulation results

Simulation shows that the magnet in ideal conditions meets the Hall Probe calibration requirements; instead when poles are skewed the homogeneity goes outside the requirements, but it can however be increased with shimming. Shimmins is a trial and error procedure but COMSOL Simulation provides guidelines on shim positioning.

4 Field mapping

We mapped the magnetic field using an NMR Probe mounted on a 2-axis motion robot, with LabVIEW interface. APPENDIX A explains the basic theory and principle of operation of the NMR Probe, focusing on the model used in this work: probe 1062 for Metrolab PT 2025 Teslameter.

4.1 Instrumentation setup

NMR Probe

[6] The NMR Probe (Figure 16) measures the magnitude of the magnetic field. It contains an active volume and an integrated amplifier for the acquisition of the NMR signal. A cable connects the probe with Metrolab PT 2025 Teslameter (Figure 17), which provides also a user interface. The result is displayed in Tesla with a resolution of 10^{-7} T but precision is minor because it depends also on several factors such as probe calibration, field magnitude and field gradient in the measured point. The average error is $\pm 5 \times 10^{-7}$ T. Each probe has a own measurement range. It is better to work with the upper part of the range because the Signal to Noise Ratio is higher than in the lower part. At the beginning it was used the NMR Probe No.5 whose range is 0.7 - 2.1 T; then we changed with NMR Probe No.4 when it became available. Probe No.4 has a range of 0.35 - 1.05 T. Since the field that had to be mapped is of 0.8 - 1.05 T, this probe is better because it works in the upper part of its measurement range. The probe active volume is 4 $mm \times 4.5$ mm; the position of its center is marked on the probe surface and is 7 mm distant from the probe tip. This information is important in order to correlate the magnetic field value with the position of the measured point. Then the NMR Probe in automatic mode can measure the magnetic field only if field gradient is minor than 350 ppm/cm for Probe No.5 and 800 ppm/cm for Probe No.4, in the lower part of their measurement range.

Figure 16: NMR Probe with cable.

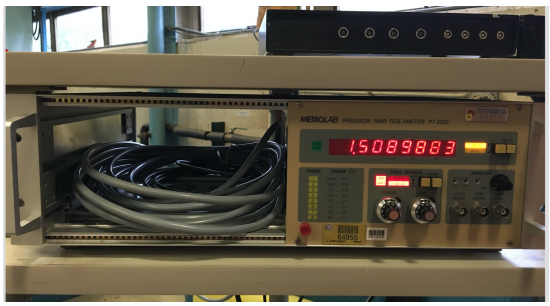

Figure 17: Metrolab PT 2025 Teslameter.

Robot

The robot (Figure 18) can move along X and Z direction by means of two step motors; it can also be manually moved along Y direction. The NMR Probe is mounted on a fixed link of the robot. At first the robot axis was aligned with the magnet axis in the magnet center so that, when the robot moves along X direction, the NMR Probe performs an horizontal line scan of the field at a constant and equal distance from the poles surface. Instead when the robot moves along Z direction, the NMR Probe performs a vertical line scan of the field and, again, at a constant and equal distance from the poles surface. Y axis

was only used in the alignment procedure: the NMR Probe is held all the time equidistant from the two poles surface.

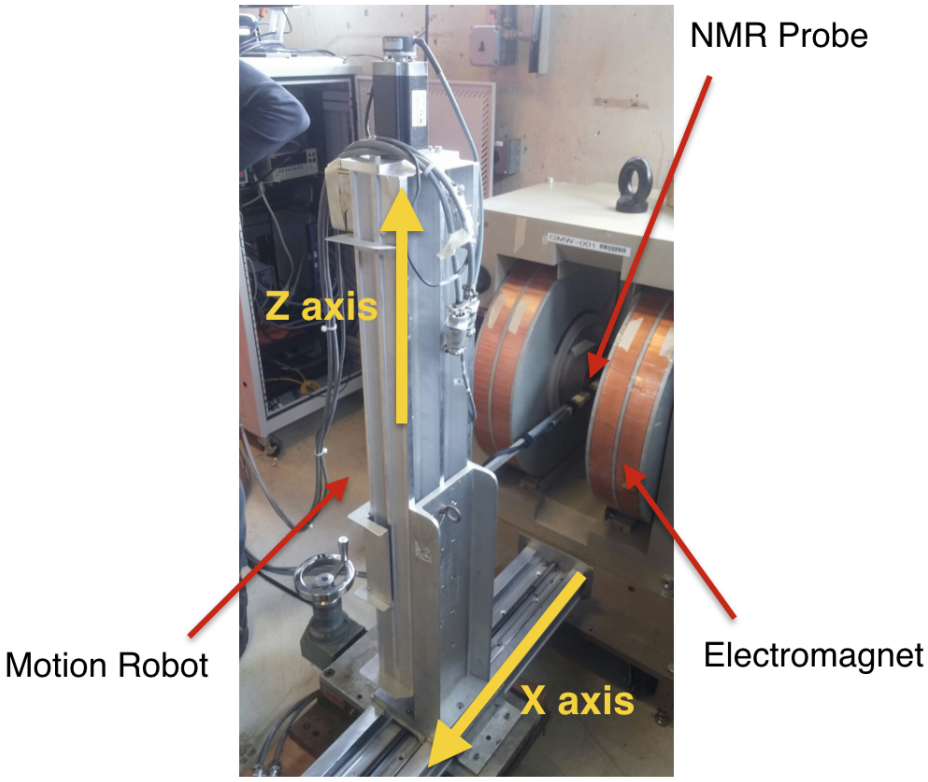

Figure 18: Robot, NMR Probe and Electromagnet setting.

Electromagnet

It is sufficiently described in Chapter 1 and modeled in Chapter 2. Remember the important difference that the magnet used in this project has coils connected in parallel; instead the characteristic curves taken from the manual and COMSOL Simulations consider coils connected in series. The effect is that at a given value of supply current, the field value in the first case is approximately half with respect to the second one.

Power Supply

The power supply used to supply current to the magnet coils is Danfysik (Figure 19). The current can be manually adjusted with fixed steps, and polarity can be inverted. Danfysik Ultrastab Saturn (Figure 20) is the current transducer used as feedback current measurement and supply current control [7]. It can ideally provide 10^{-6} supply current stability (relative value).

Water cooling system

A water cooling system is used to cool both the power supply and the magnet coils in order to avoid an excessive heating when the magnet is turned on. The control panel (Figure 21) monitors the cooling water temperature: if the pump return water temperature goes over the threshold, the control system will open the valve that activates the external water recycle. Providing additional water, the external recycle limits the cooling water temperature; in that way, a high heat exchange efficiency is held and then the magnet and power supply temperature are limited. It was noted that the pump return water and coil temperature go in a stable condition around the threshold. This is an important aspect because increasing the threshold, the magnet and power supply work in a high temperature state.

Figure 19: Power supply.

Figure 20: Feedback supply current transducer.

Figure 21: Cooling water temperature control panel.

Multimeters

At first Keithley Model 2001 Multimeter (Figure 22) was used to measure, with a precision of 10^{-5} V, a voltage proportional to the supply current [8]. Then it was replaced by Agilent 3458A Multimeter (Figure 23) which increases the precision up to 10^{-6} V [9]. Further Hp 3457A (Figure 24), a multimeter with a precision of 10^{-4} V, was used to measure the power supply voltage [10].

Figure 22: Keithley Model 2001 Multimeter.

Figure 23: Agilent 3458A Multimeter.

Figure 24: Hp 3457A Multimeter.

4.2 LabVIEW Interface

LabVIEW (Laboratory Virtual Instrument Engineering Workbench) interface was used to move the robot and read the measurement field value from the NMR Probe. LabVIEW is a system-design platform and development environment for a visual programming language from National Instruments [12].
Figure 25 shows the control panel of the robot movement interface. The robot can be moved along X and Z axis setting the number of steps (it was measured that the ideal length of one step is 12.7 μm). Robot position and past trajectory in the XZ plane can be visualized on the screen. Knowing the initial position of the NMR Probe sensitive region and the actual robot position, the position of each point in which the field measurement was performed could be easly deduced.

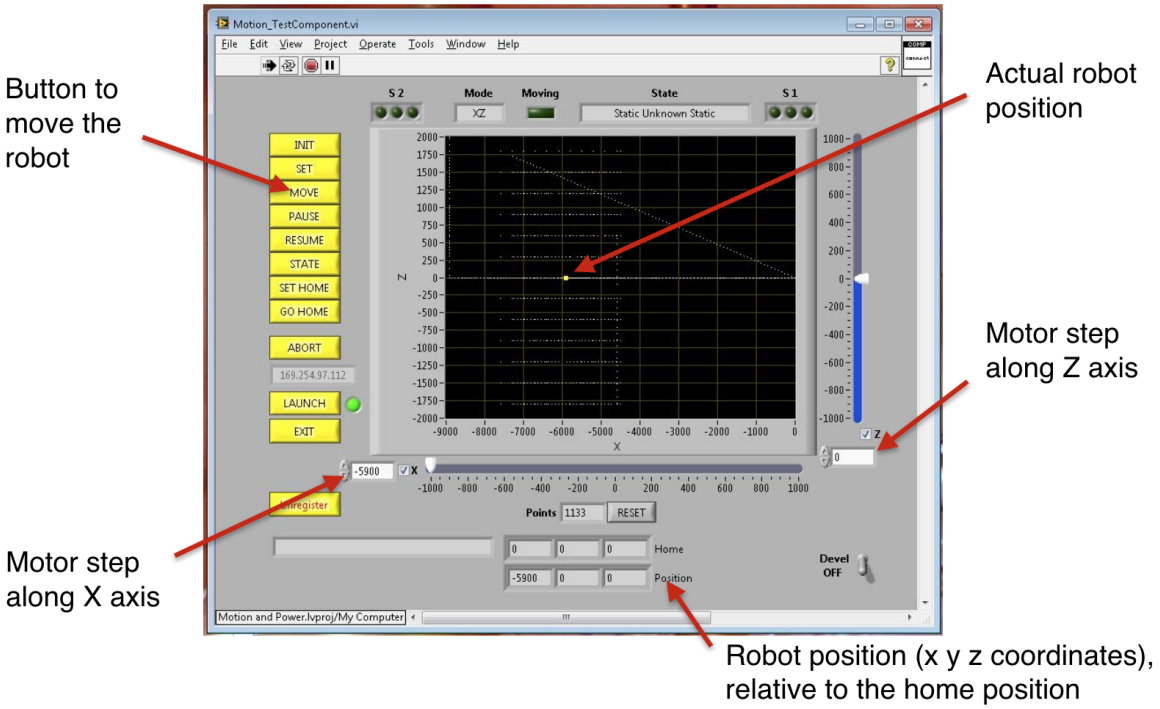

Figure 25: Control panel of the robot movement interface.

Figure 26 shows the control panel of the NMR Probe reading interface. The measured field value is visualized on the screen and can be saved in a spreadsheet file. The automatic searching mode makes a coarse scan of the entire measurement range; when it passes around the actual field value a light flashes at the left of the display. Then the teslameter makes a finer field scan; when the NMR Probe has finally locked the field, the light stays on. Now the field value read on the screen is consistent. When the field gradient is higher than the limit shown above, the automatic mode is not able to lock the field. In this case it is suggested to use the manual searching mode in order to do however the measurement, even though with a lower precision.

These interfaces were already existing. After learning LabVIEW programming basics, the block diagrams of these two programs were studied and combined in order to work together: that is read the field value and the position of each measured point.

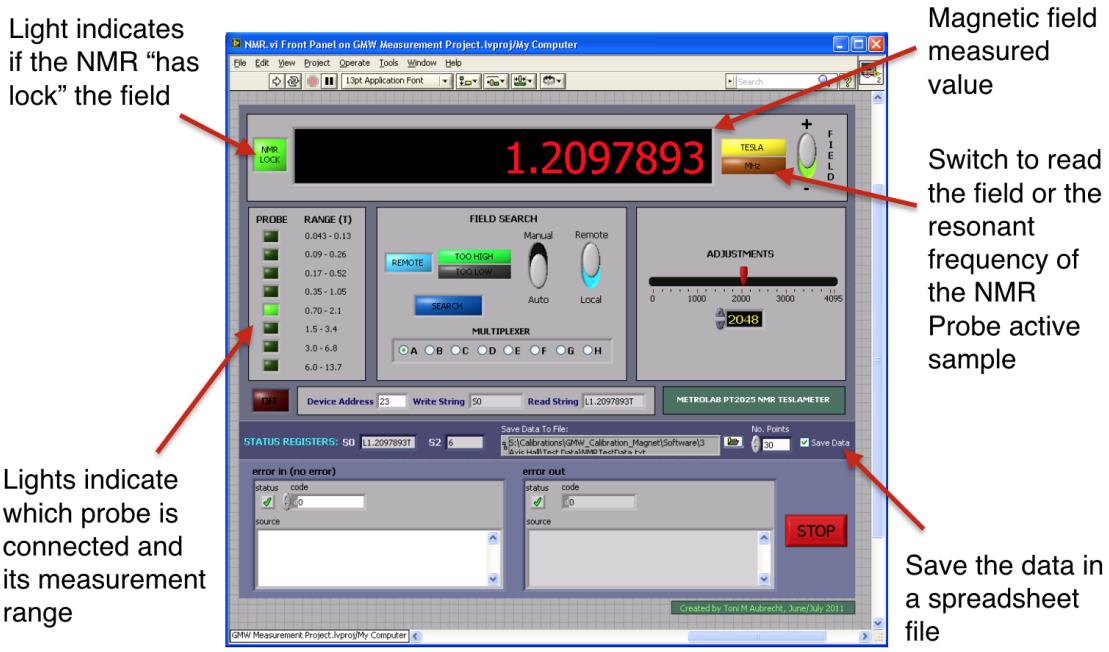

Figure 26: Control panel for the NMR Probe reading.

4.3 Results

1D Field Mapping

At first a coarse field scan (Figure 27) along the X axis in the magnet center (Z = 0) was performed with a resolution of 6.35 mm (step size 500 in X movement), using the NMR Probe No.5. Supply current was set to 100 A. The plot shows that maximum field value is not in the magnet center (as instead expected in the ideal case) and the homogeneity over 2 cm is about 10^{-4} T. Only a small region can be measured because Probe No.5 is insensitive if field gradient is larger than 350 ppm/cm.

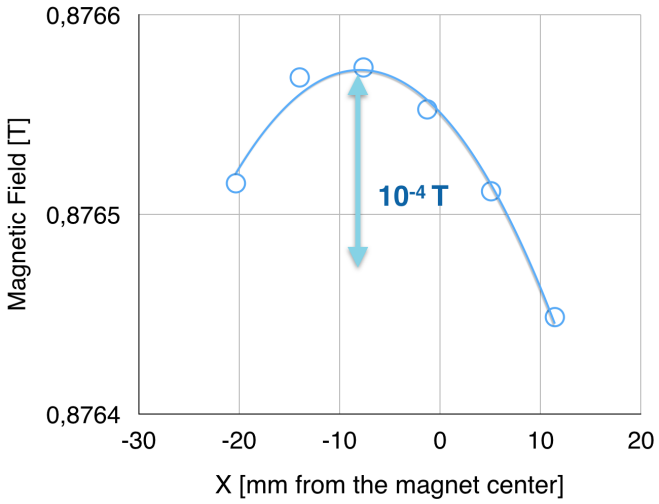

Figure 27: Coarse field scan along X axis (Z = 0) with 100 A supply current, performed with Probe No.5.

Then a finer field scan (Figure 28) was done along the same axis, using a resolution of 1.27 mm and 120 A of supply current. Again the field maximum value is not in the center and homogeneity over 2 cm is about 10^{-4} T.

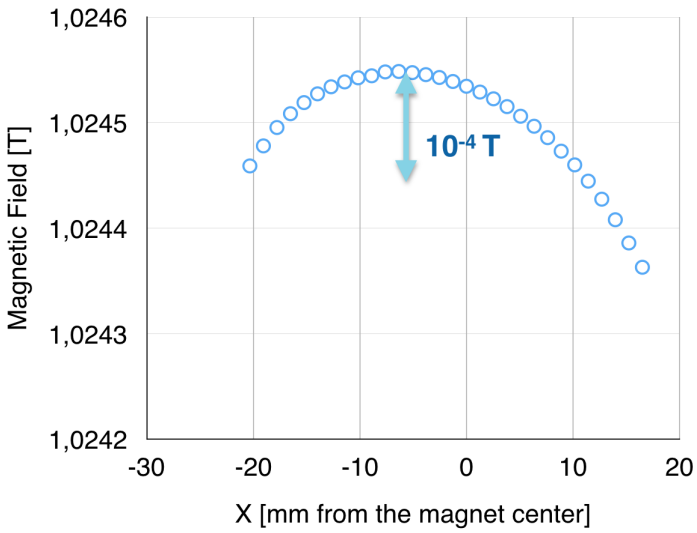

Figure 28: Fine field scan along X axis (Z = 0) with 120 A supply current, performed with Probe No.5.

2D Field Mapping

A 2D field mapping of the central plane XZ was performed with a resolution of 3.81 mm (step size 300 in X and Z movement), at three different values of supply current: 80 A, 100 A and 120 A, using NMR Probe No.4. The measured region is 38.1 mm × 38.1 mm.
In each case the same 2D plot is shown from two different views: on the left the surface height is proportional to the field magnitude in the corresponding XZ coordinate. In this way it is graphically intuitive compare the field differences over the plane, with a fixed scale (5×10^{-4} T). Instead on the right, the surface view from the top, with color proportional to the field magnitude, makes graphically simpler the analysis of the field distribution over the plane. Then the most homogeneous 2 cm × 2 cm region of each plane is highlighted with a blu square. Note also that in each case the scale is obviously different, but the differences between the upper and the lower scale values are the same (10^{-3} T) in order to make possible a graphical comparison of field homogeneity between these three different cases. Table 1 compares the numerical results of these maps.

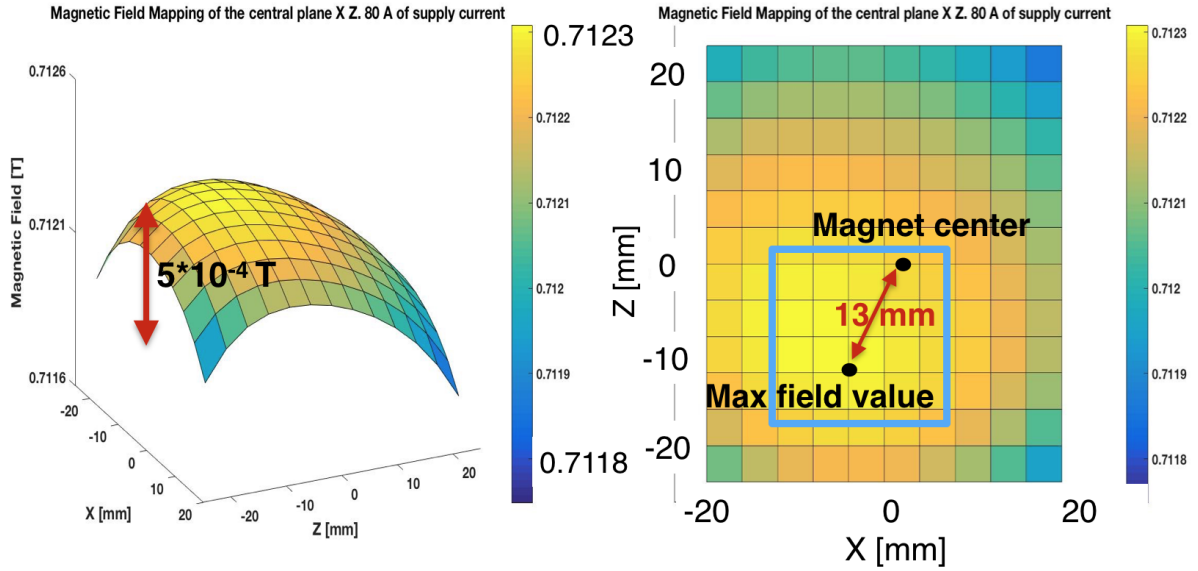

Figure 29: 2D field map of the central plane XZ with 80 A supply current, performed using Probe No.4.

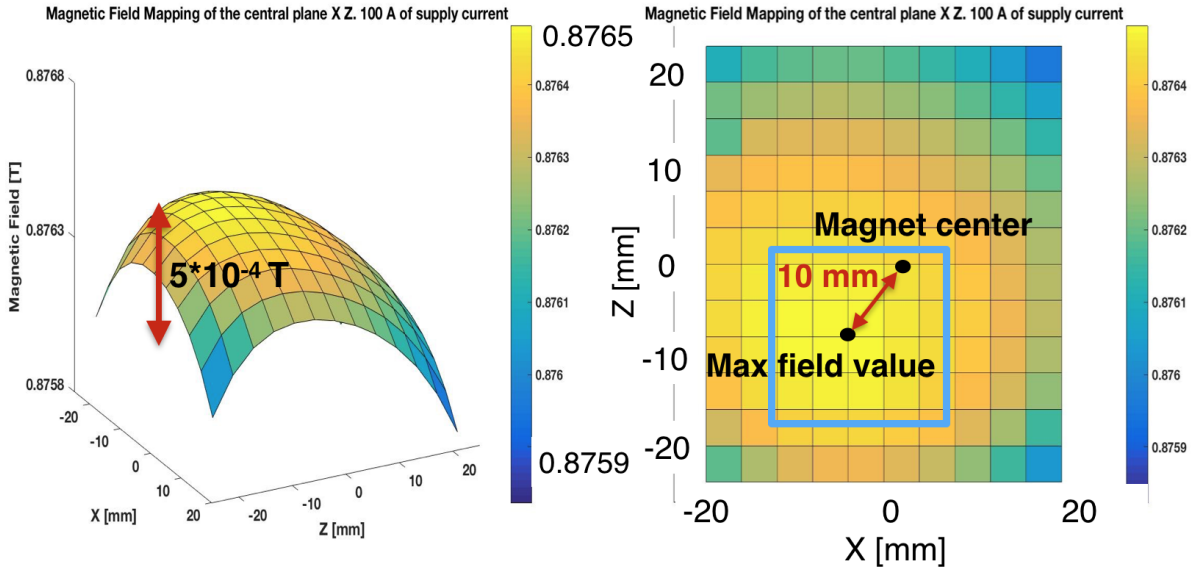

Figure 30: 2D field map of the central plane XZ with 100 A supply current, performed using Probe No.4.

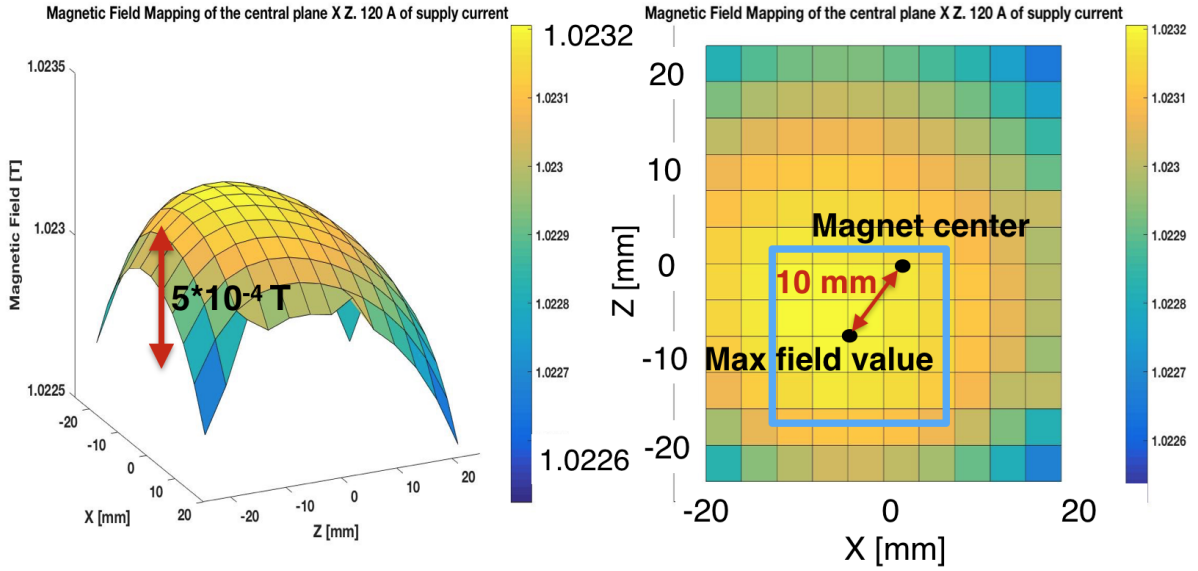

Figure 31: 2D field map of the central plane XZ with 120 A supply current, performed using Probe No.4.

Supply current [A]	80	100	120
Field homogeneity over the entire plane [10^{-4} T]	5.6	6.7	7.0
Field homogeneity over 2 cm $\times$ 2 cm region [10^{-4} T]	1.3	1.5	1.4
Max field value [T]	0.712308	0.876482	1.023206
Distance between the max field value and the magnet center [mm]	13	10	10

Table 1: Comparison of numerical 2D field mapping results with three different current values.

Increasing the supply current, the field homogeneity over the entire plane gets worse, but it is almost the same over the 2 cm × 2 cm region of interest. There is also an evident distance between the point where there is the maximum field value and the magnet center, as previously seen from the 1D field map.

2D Field Mapping with pole spacers

How suggested by COMSOL Simulations, the asymmetric field distribution around the magnet center could be due to pole skewness. For this reason, we used three pole spacers of the same length (50 mm) blocked between the poles surface (Figure 32), in order to align the poles and reduce the skewness. It is a rudely method but how shown below, it has produced good results. Pole spacers limit the movement of the NMR Probe along the entire XZ plane in the magnet center. However it is shown in the previous plot that only a small region of the plane (38.1 mm 38.1 mm) can be mapped due to the field gradient. Since in this measurable region pole spacers do not limit the movement, they are not a problem for the field mapping.

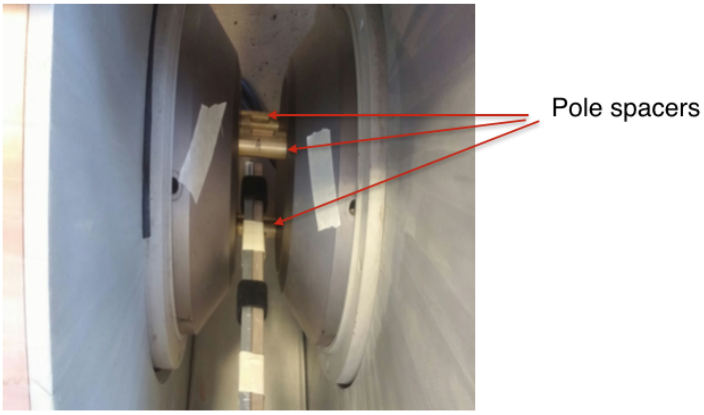

Figure 32: Pole spacers blocked between the poles surface.

Figure 33 shows the 2D field map with the use of pole spacers. The field distribution is more symmetric around the magnet center and the homogeneity is increased from 1.4×10^{-4} T to 8.8×10^{-5} T over 2 cm × 2 cm region. The maximum field value is nearer the center with respect to the previous case without the spacers.

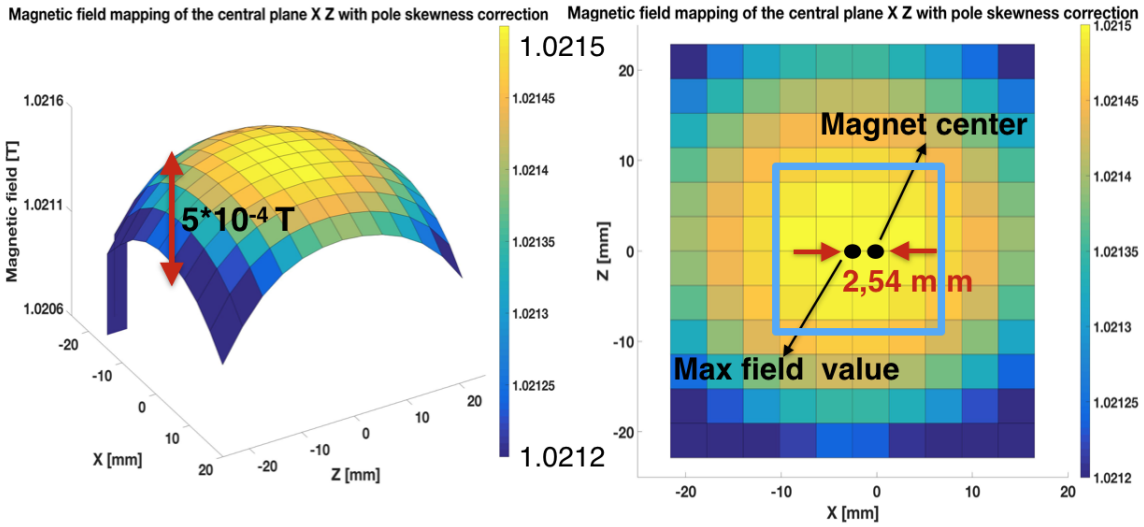

Figure 33: 2D field map of the central plane XZ with 120 A of supply current, performed with Probe No.4. Skewness reduction using pole spacers.

Magnetic Hysteresis

Performing several field mappings a field variation of the order of 10^{-3} T was observed between the same points of maps of different days. Since between two different days the magnet was turned off, it was possible that this variation could be due to magnetic hysteresis.

Hysteresis is the system dependence on the present and past input. The history of the state assumed by the system affects the behavior of the present state. In a ferromagnetic material, when an external magnetic field is applied, the atomic dipoles align themselves with it. When the external field is removed, part of the alignment will be retained and the material holds a magnetization (Figure 34) [15].

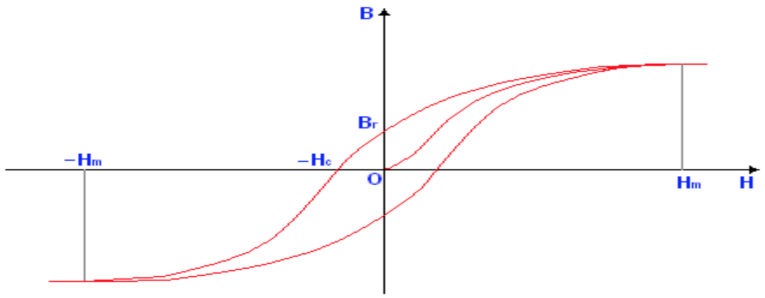

Figure 34: Typical hysteresis curve in a ferromagnetic material. When an external H field is applied, the material magnetizes up to a max saturation value. When the external field H is removed, the total magnetic field B is not zero because the material holds a magnetization.

The hysteresis curve of the magnet (Figure 35) was performed measuring the field in the magnet center (X = 0, Z = 0) and using probe No.4. At first it was applied a negative supply current of -120 A; the current was increased up to 120 A using fixed steps of 10 A. Then it was decreased again to -120 A using the same steps. The curve shows that the field difference between the upward curve and the downward curve is about 10^{-2} T.

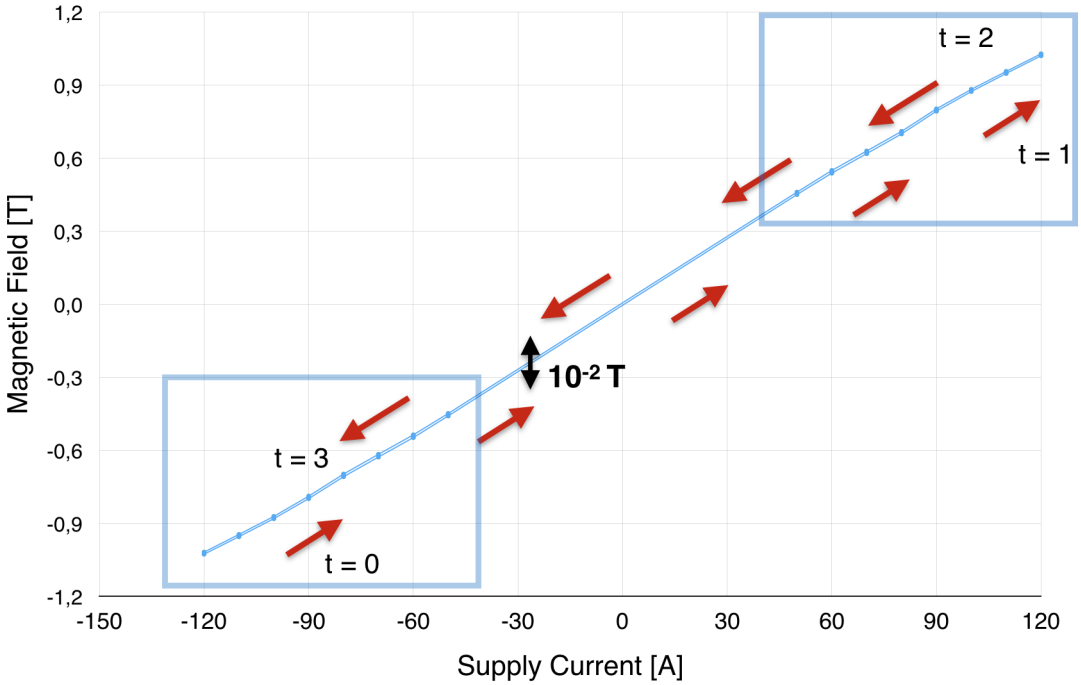

Figure 35: Hysteresis curve of the magnet. Only the two regions highlighted with blue rectangle could be measured because near the curve center the field is lower and it is outside the Probe No.4 measurement range.

Figure 36 shows a zoom of the two highlighted regions of the hysteresis curve in order to observe better the difference between the upper and lower line.

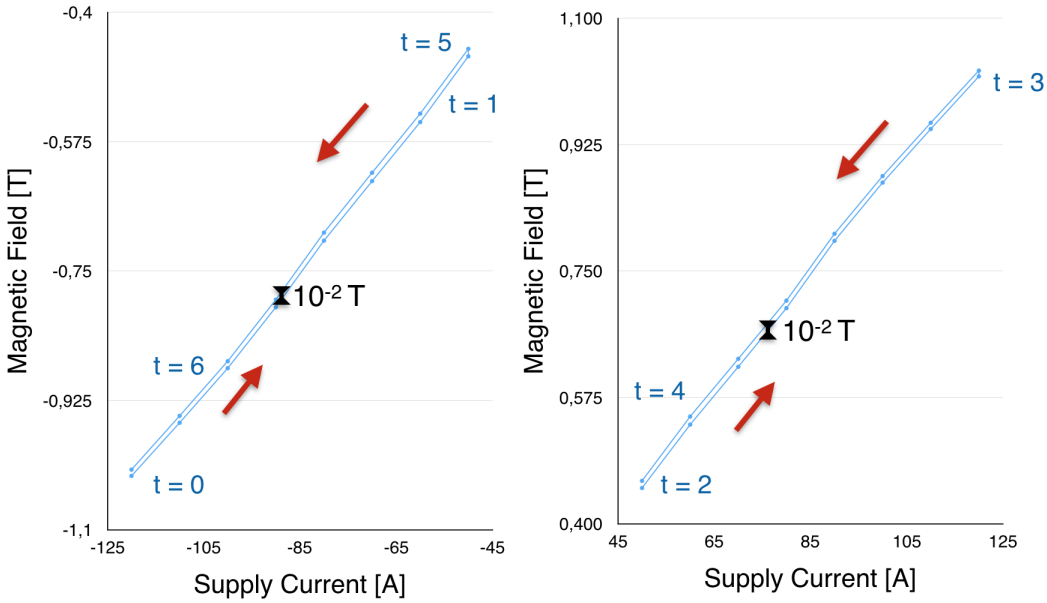

Figure 36: Zoom of the two measured regions of the hysteresis curve of the magnet.

To avoid that the history of the state assumed by the magnet can influence the actual measurement, a degaussing procedure can be used: it helps to remove the permanent magnetization before applying the desired supply current for the actual measurement. The degaussing procedure (Figure 37) consists in applying at first a positive high magnetic field on the material in order to magnetize it at the maximum value; at second inverting the polarity of the external field, magnetizing the material in the opposite direction; then repeating this two steps decreasing the magnitude of the external field, down to zero after several cycles.

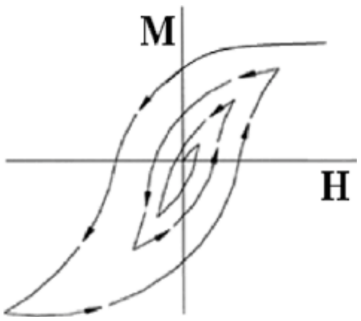

Figure 37: Degaussing procedure.

Field Vs Supply Current

It was performed the measurement of the magnetic field in the magnet center (X = 0, Z = 0) increasing the supply current from 0 A up to 120 A with fixed step of 10 A (Figure 38), using NMR Probe No.4. Only the magnetic fields generated by supply current higher or equal than 50 A were within the probe measurement range. However this is sufficient to find a linear correlation between field and supply current. The first six points are well fitted by a line with an angular coefficient of 0.0084 T/A. The last two points are under this fitting line: this is due to the beginning of iron saturation. In fact, the magnetization of a ferromagnetic material increases with the applied external magnetic field up to a maximum limit; over this limit, the magnetization can no longer increase, even if the external field increases [16].

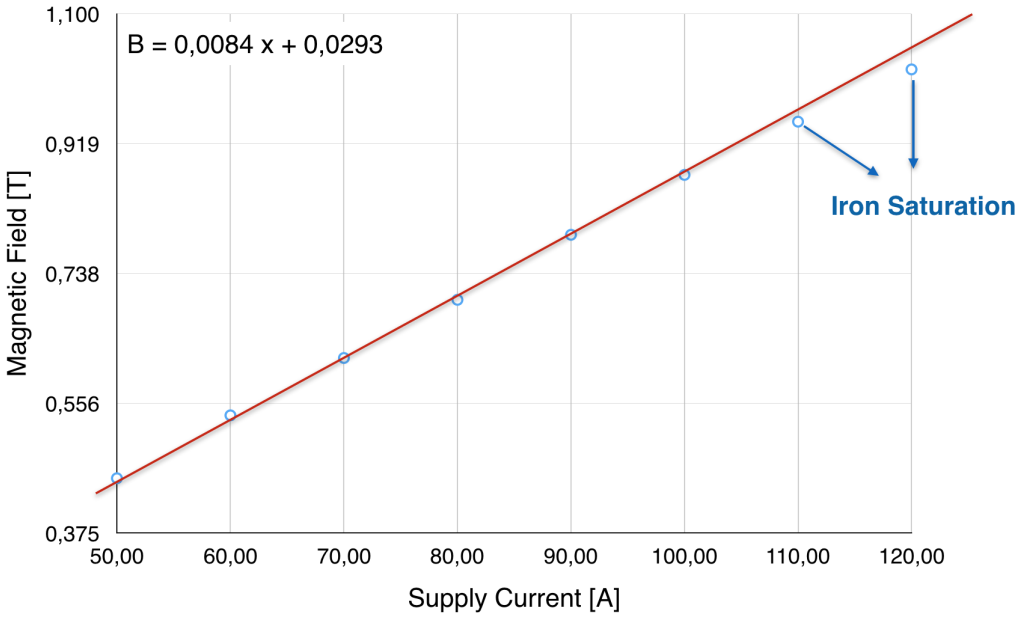

Figure 38: Field Vs supply current.

Field repeatability over time

The field repeatability over time was studied repeating several times the field measurement with 80 A of supply current. Since the magnet can not be always hold on, the field stability must be guaranteed also each time the magnet is turned on. In other words we wanted to see if the magnet can generate the same field each time it is turned on with the same supply current. We applied the degaussing procedure to remove the residual permanent magnetization, we set the current from 0 to 80 A and we measured the field. Then these three steps were repeated several times. The result, shown in Figure 39, is that the field repeatability is about 10^{-3} T.

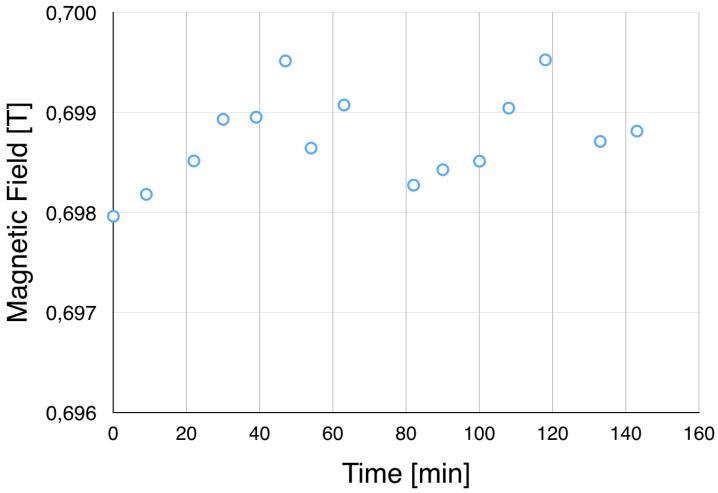

Figure 39: Field repeatability over time with cooling water temperature set point of 85 F.

This field variation is not due by hysteresis because the degaussing procedure was applied before doing each measurement. The supply current read by the multimeter during the test does not change enough to explain this field difference.
This test was done using 85 F as cooling water temperature set point. We tried to increase the set point up to 100 F and we repeated the test. At the beginning, the field variation over time was as the

previous one but, after 45 minutes the field became more repeatable, up to 10^{-4} T over almost two hours (Figure 40). Note that in figure, the last two points were taken without doing the degaussing procedure before applying 80 A of supply current; the field variation of these two points with respect to previous is due to hysteresis.

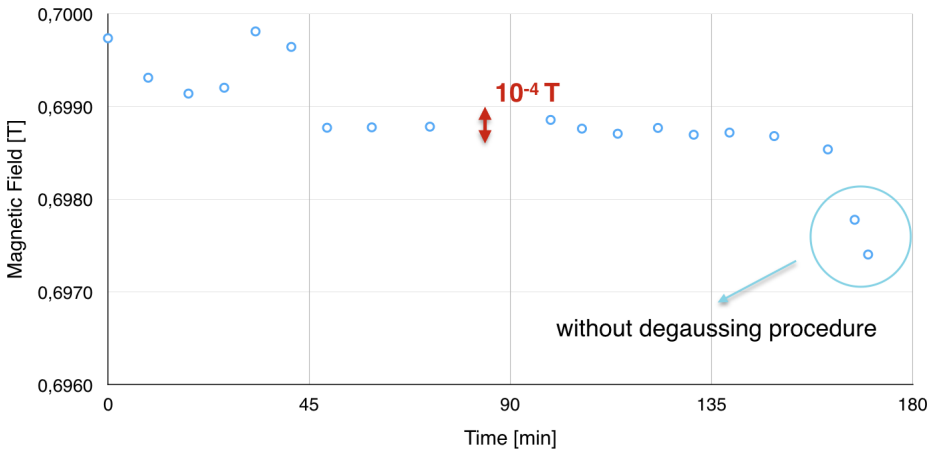

Figure 40: Field repeatability over time with cooling water temperature set point of 100 F.

Field stability over time

Then it was studied the field stability over time (about 6 hours), holding the magnet always on during the test. The test was repeated two times in two different days. The result is a field stability of 10^{-5} T over time.

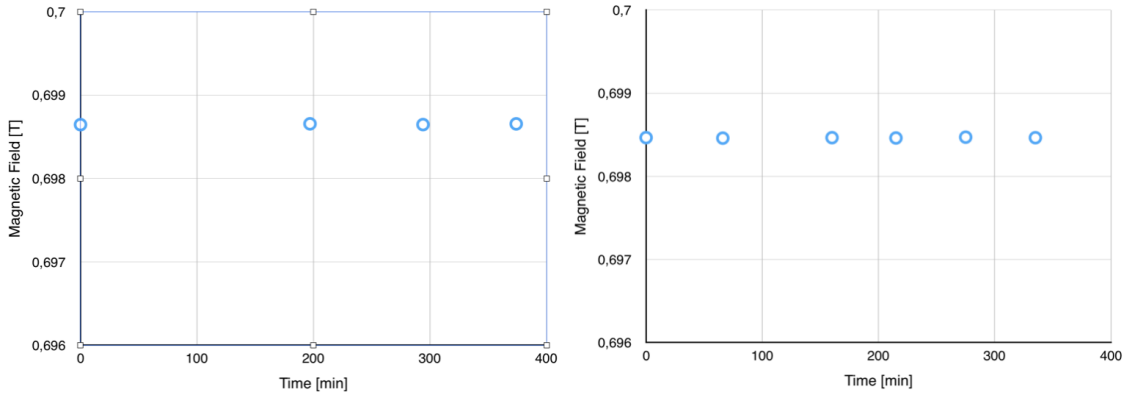

Figure 41: Field stability over time with cooling water temperature set point of 100 F, with the magnet held always on.

4.4 Field mapping discussion

Repeating the field mapping several times with the same supply current, a field variation of 10^{-3} T was observed between maps of two different days. Since in the measurements the degaussing procedure was not performed before applying the desired current, a possible explanation of the field variation could be the hysteresis effect. So we studied the magnetic hysteresis and we found that effectively there is a difference of 10^{-2} T between the upward and downward curves, that can explain the field variation over two different maps. However measuring the field several times with 80 A of supply current applying each time a degaussing procedure before going up to 80 A, we found just the same variation of 10^{-3} T and this could not be due by hysteresis effect. Between different measurements, the current sensor measured

small variations in the supply current, but not high enough to explain the field variation of 10^{-3} T. Using the field Vs current plot we can in fact deduce the current variation needed to produce a certain field variation. So what is the cause of this field variation ? When the power supply is set at a certain current value, it reaches the desired current value following a non linear trajectory. If the current is increased very quickly, the power supply can exhibit an overshoot; in this way it reaches the desired value from the top of the field Vs current plot, not from the bottom. So there was still the hysteresis effect influencing the measurements. Furthermore, we wanted to see if temperature could influence the field stability. Increasing the water cooling system temperature set point up to 100 F, ramping to the desired supply current plateau very slowly and applying a degaussing procedure before doing each measurement, the test at 80 A exhibited smaller field variations, of 10^{-4} T. Combining these three methods the field repeatability increased, but why are still there field variations of 10^{-4} T ? The current sensor still showed the presence of small current variations, however not large enough to explain the field variation. We trust the field value read by the NMR Probe because it is reliable and recently calibrated. The most logical explanation of this phenomena is that the supply current sensor did not measure the real supply current. So, although we read a stable supply current over time, actually the power supply did not provide a current as stable over time. Each time the magnet was turned on and set to the same supply current value, actually the current provided was different. The cause of this problem lied in the supply current control done by the Danfysik Ultrastab Saturn current transducer. It is not able to hold a current stability of 10^{-6} (relative value) as described by the manual, but only of about 10^{-4} with high temperature and 10^{-3} with low temperature, due to some wrong cable connections. Since the supply current sensor is connected to this current transducer, it does not show the existence of power supply variations.
Instead if the magnet is hold on with 80 A of supply current, the field stability over time is about 10^{-5} T if we use the temperature set point of 100 F. It is a good result because it meets the requirement for the Hall Probe calibration in term of stability over time. The problem that still remains is the repeatability of the calibration: for this purpose it is needed to increase the present repeatability over 10^{-4} T. To achieve this goal one has to work on improving the power supply control.
Regarding the field homogeneity over space, using the pole spacers we measured a homogeneity of 8.8×10^{-5} T over 2 cm $\times$ 2 cm region, not good enough for the Hall Probe calibration but improvable with a shimming procedure.

5 Conclusions

Simulations of the magnetic field generated by a model of the electromagnet GMW 3474, show that the magnet can meet the Hall Probe calibration requirements in the ideal case; instead, a non ideality as pole skewness decreases the field homogeneity but a good shimming procedure can however increase again the homogeneity.
Testing the actual magnet we found that the field homogeneity over 2 cm $\times$ 2 cm region needed for the Hall Probe calibration is 8.8×10^{-5} T after a pole alignment with pole spacers. It is a well result but not good enough for the Hall Probe calibration; however it can be improved with a shimming procedure. Currently we can not go over a field repeatability of 10^{-4} T over time because the power supply stability is limiting the test. The field stability over time is 10^{-5} T and meets the Hall Probe calibration requirements. Shimming procedure can potentially increase the field homogeneity but it was not done because first one has to work on controlling the power supply: not only do we need homogeneity over the mapped volume, but also over the time of the hall probe calibration and over different days to ensure repeatability of the measurement.
We are confident that finally one can achieve the values needed for the Hall Probe calibration.

6 References

Articles

[1] Fermi National Accelerator Laboratory, October 2014, *Mu2e Technical Design Report.*
[2] 2M. Tartaglia, S. Feher, February 2016, Mu2e-doc-1275, *Mu2e Field Mapping System.*
[3] L. Elementi, S.Feher, H. Fredsam, C. Orozco, T. Strauss, Mu2e-doc-6694, *Hall Probe Calibration Equipment.*
[4] S. Feher, *FMS Hall Probe Calibration Strategy.*

Manuals

[5] GMW, *User's Manual Model: 3474-140 250MM Electromagnet*, Revision Date: July 2009.
[6] Metrolab Instrument, *PT 2025 NMR Teslameter User's Manual*, Version 2.0 (Revision 1.0), September 2003.
[7] Danfysik, *Ultrastab Saturn Current Transducer User Manual*, April 2007.
[8] Keithley, *Model 2001 Multimeter Operator's Manual*, Revision Date: February 2009.
[9] Agilent, *3458A Multimeter Data Sheet.*
[10] Hp, *3457A Multimeter Service Manual*, February 1988.

Link

[11] https://en.wikipedia.org/wiki/Nuclear_magnetic_resonance
[12] https://en.wikipedia.org/wiki/LabVIEW
[13] http://www.ni.com/labview/i/
[14] https://en.wikipedia.org/wiki/COMSOL_Multiphysics
[15] https://en.wikipedia.org/wiki/Hysteresis
[16] https://en.wikipedia.org/wiki/Saturation_(magnetic)

Appendix A

Basic theory and principle of operation of the NMR Probe for PT 2025 Teslameter

Basic theory of NMR (Nuclear Magnetic Resonance) All nucleons, composing any atomic nucleus, have the intrinsic quantum property of **spin**. The overall spin of the nucleus is determined by the *spin quantum number* **S**. Using the classical theory, for a particle the spin is like performing a rotation around own axis which it is associated an angular momentum. The **angular momentum** associated with the nuclear spin has a quantized magnitude and orientation. When an external magnetic field along a z direction is applied, the angular momentum component along the z axis is:

$$P_z = m\hbar$$

where $\hbar$ is the reduced Planck constant and **m** is the *magnetic quantum number*, that can take values from $-S$ to S in integer steps. In the following description are considered nuclei with $S = 1/2$ because NMR Probe uses the property of Hydrogen atoms whose have a nuclear spin $S = 1/2$. A charge particle with spin property, as a proton of the Hydrogen nucleus, has a **magnetic moment**. The relation between the magnetic moment and the angular momentum is described by γ, the **gyromagnetic ratio**:

$$\mu_z = \gamma P_z = \gamma m\hbar.$$

In a nucleus with $S = 1/2$, m can take only two values (-1/2, 1/2): the nucleus has only two energy states, one with **parallel** magnetic momentum ($S = 1/2$) and the other **antiparallel** ($S = -1/2$) to the external magnetic field direction. The energy of a magnetic momentum in the presence of an external magnetic field is:

$$E = -\mu \cdot B_0 = -\mu_z B_0 = -\gamma m\hbar B_0$$
$$\Delta E = \gamma\hbar B_0$$

Parallel state is more stable than antiparallel state, so a larger number of nuclei have a magnetic moment parallel with the external field and a smaller number are antiparallel. When an external electromagnetic radiation with a frequency of

$$\nu_0 = \frac{\Delta E}{h} = \frac{\gamma B_0}{2\pi} \quad \text{(Larmor frequency)}$$

is applied, nuclei absorb energy and from the lower energy state they go up in the higher energy state. Larmor frequency is linearly proportional to the external magnetic field but depends also on the material. For protons ^{-1}H, γ is known very precisely:

$$\gamma = 42.57608 \ MHz/T.$$

This means that for magnetic field of the order of 1 T, NMR frequencies lie in the radio frequency region.

Principle of operation of the NMR Probe for PT 2025 Teslameter The NMR Probe has an active sample rich of hydrogen atoms (a solid sample or heavy water), wound by flat radio frequency coils. When the sample is placed inside an external magnetic field and coils generate an electromagnetic field at the sample resonance frequency, the nuclei of the sample absorb energy. With the energy absorption, the difference between the population of the two energy states is reduced. However the equilibrium is re-established because nuclei in the high energy state relaxed due to the spin-lattice interaction. For

this reason protons continuously absorb energy from the alternating field if there is applied the Larmor frequency. A typical way to increase the absorption is to keep the equilibrium to the lower energy state side, adding a paramagnetic salt in the sample that reduce the spin-lattice relaxation time.

Since the active sample is the inductor inside the coil, the continuous energy absorption causes the reduction of the quality factor Q of the coils.

The resonance frequency of protons is modulated applying a low frequency ($30 - 70$ Hz) triangular wave modulating magnetic field, parallel to the external field B_0. If the radio frequency is close enough to the nuclear resonance frequency corresponding to the main field B_0, an absorption signal (amplitude reduction of the radio frequency voltage across coils) appears every time the resonance is crossed due to field modulation. This signal is amplified in the probe integrated amplifier and transmitted to the PT 2025. A control system measure a voltage proportional to the modulating magnetic field at the instant when nuclear magnetic resonance occurs and modify the radio frequency in such a way that nuclear resonance occurs exaclty at the zero crossing of the modulation. In this way the radio frequency is linear proportional to the external field B_0 as without the modulation. So B_0 can be easly calculated:

$$B_0 = \frac{2\pi\nu_0}{\gamma}.$$

Because of the weakness of the NMR signal, the radio frequency voltage must be extremely clean with respect to any spurious amplitude or frequency modulation and noise; otherwise the signal-to-noise ratio (SNR) becomes poor. When the magnetic field to be measured is not homogeneus but there is a gradient, different region of the active sample are not subjected to the same field and for this reason the SNR is lower.

In the search operating mode the frequency counter of PT 2025 performs a coarse scan of the entire frequency range; when the NMR Signal appears, a finer scan around the current frequency is performed to lock the field at the correct value. In this mode of operation the field value can be locked if the field gradient is lower than a certain value depending on the NMR Probe.

Figure A.1 shows the field range of each NMR Probe for PT 2025 Teslameter: we were interested in magnetic field of about 1 T so Probe No.4 and No.5 were appropriate for this work. Figure A.2 shows the maximum field gradient for each probe over which the SNR is too small to lock the correct field value in the automatic searching mode. Note that Probe No.4 is more suitable for less homogeneous field than Probe No.5: measuring field of about 1 T, Probe No.4 works in the upper level of its measurement range, where the max field gradient is 1500 ppm/cm; instead Probe No.5 works in the lower level of its measurement range where the max field gradient is 350 ppm/cm.

The result is displayed by the PT 2025 in Tesla with a resolution of 10^{-7} T or in frequency with a resolution of 1 Hz. Due to instrument accuracy we were confident in a resolution of 10^{-6} T that is however good enough for our work.

Despite the fact that the NMR probe gives a precise field or frequency reading independent of orientation, it would be better if the NMR Probe is placed inside the external magnetic field with a certain orientation: the radiofrequency coil axis perpendicular to the external magnetic field direction in order to maximize the absorption and then improve the NMR Signal; the modulating magnetic field parallel to the external magnetic field direction.

Probe N°	Field Range (Tesla)	Probe Type	Frequency Range (MHz)	Active Volume (Diam x L (mm)
1	0.043 to 0.13	^{1}H	1.9 to 5.6	7 x 4.5
2	0.09 to 0.26	^{1}H	3.8 to 11.2	5 x 4.5
3	0.17 to 0.52	^{1}H	7.5 to 22.5	4 x 4.5
4	0.35 to 1.05	^{1}H	15.0 to 45.0	4 x 4.5
5	0.70 to 2.1	^{1}H	30.0 to 90.0	4 x 4.5
6*	1.5 to 3.4	^{2}H	7.5 to 22.5	4 x 4.5
7*	3.0 to 6.8	^{2}H	15.0 to 45.0	4 x 4.5
8*	6.0 to 13.7	^{2}H	30.0 to 90.0	4 x 4.5

Figure A.1: Measurement range of NMR Probe for PT 2025 Teslameter

Probe N°	Field Range		
	High	Middle	Low
1	600	900	600
2	1200	1600	1200
3	1200	1400	1400
4	1500	900	800
5	250	600	350
6	240	280	280
7	300	180	160
8	50	120	70

Figure A.2: Maximum field gradient for each NMR Probe